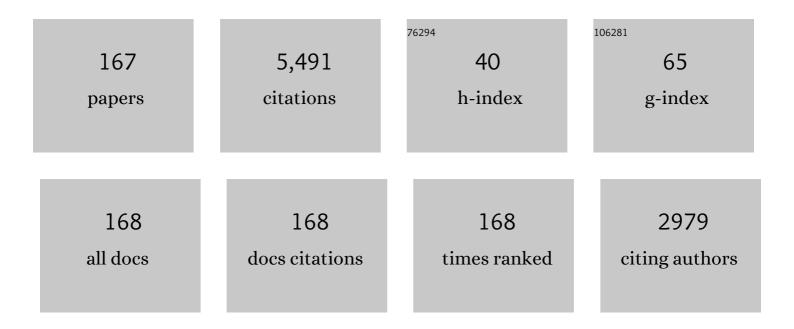
## Yongchen Song

List of Publications by Year in descending order

Source: https://exaly.com/author-pdf/7116256/publications.pdf Version: 2024-02-01



#	Article	IF	CITATIONS
1	Hydrogen production from the thermochemical conversion of biomass: issues and challenges. Sustainable Energy and Fuels, 2019, 3, 314-342.	2.5	224
2	Enhanced CH 4 recovery and CO 2 storage via thermal stimulation in the CH 4 /CO 2 replacement of methane hydrate. Chemical Engineering Journal, 2017, 308, 40-49.	6.6	207
3	Mechanical behavior of gasâ€saturated methane hydrateâ€bearing sediments. Journal of Geophysical Research: Solid Earth, 2013, 118, 5185-5194.	1.4	189
4	Numerical simulation of gas recovery from a low-permeability hydrate reservoir by depressurization. Applied Energy, 2019, 250, 7-18.	5.1	162
5	Highly Saltâ€Resistant 3D Hydrogel Evaporator for Continuous Solar Desalination via Localized Crystallization. Advanced Functional Materials, 2021, 31, 2104380.	7.8	122
6	Water Contact Angle Dependence with Hydroxyl Functional Groups on Silica Surfaces under CO <sub>2</sub> Sequestration Conditions. Environmental Science & Technology, 2015, 49, 14680-14687.	4.6	115
7	Hydrate reformation characteristics in natural gas hydrate dissociation process: A review. Applied Energy, 2019, 256, 113878.	5.1	115
8	Flexible and Mildew-Resistant Wood-Derived Aerogel for Stable and Efficient Solar Desalination. ACS Applied Materials & Interfaces, 2020, 12, 28179-28187.	4.0	114
9	Effect of fuel origin on synergy during co-gasification of biomass and coal in CO2. Bioresource Technology, 2016, 200, 789-794.	4.8	111
10	Highly Thermally Insulated and Superhydrophilic Corn Straw for Efficient Solar Vapor Generation. ACS Applied Materials & Interfaces, 2020, 12, 16503-16511.	4.0	108
11	Mechanical Characteristics of Hydrate-Bearing Sediment: A Review. Energy & Fuels, 2021, 35, 1041-1057.	2.5	108
12	A Review on Research on Replacement of CH4 in Natural Gas Hydrates by Use of CO2. Energies, 2012, 5, 399-419.	1.6	107
13	Visualization and Measurement of CO <sub>2</sub> Flooding in Porous Media Using MRI. Industrial & Engineering Chemistry Research, 2011, 50, 4707-4715.	1.8	101
14	Mechanical behaviors of permafrost-associated methane hydrate-bearing sediments under different mining methods. Applied Energy, 2016, 162, 1627-1632.	5.1	101
15	Cementation Failure Behavior of Consolidated Gas Hydrateâ€Bearing Sand. Journal of Geophysical Research: Solid Earth, 2020, 125, e2019JB018623.	1.4	94
16	Microstructure Evolution of Hydrateâ€Bearing Sands During Thermal Dissociation and Ensued Impacts on the Mechanical and Seepage Characteristics. Journal of Geophysical Research: Solid Earth, 2020, 125, e2019JB019103.	1.4	90
17	A comparative analysis of the mechanical behavior of carbon dioxide and methane hydrate-bearing sediments. American Mineralogist, 2014, 99, 178-183.	0.9	88
18	Numerical modeling for the mechanical behavior of marine gas hydrate-bearing sediments during hydrate production by depressurization. Journal of Petroleum Science and Engineering, 2019, 177, 971-982.	2.1	85

#	Article	IF	CITATIONS
19	Microstructure Observations of Natural Gas Hydrate Occurrence in Porous Media Using Microfocus X-ray Computed Tomography. Energy & Fuels, 2015, 29, 4835-4841.	2.5	81
20	Experimental research on the mechanical properties of methane hydrate-bearing sediments during hydrate dissociation. Marine and Petroleum Geology, 2014, 51, 70-78.	1.5	78
21	New Approach for Determining the Reaction Rate Constant of Hydrate Formation <i>via</i> X-ray Computed Tomography. Journal of Physical Chemistry C, 2021, 125, 42-48.	1.5	73
22	Behaviors of CO <sub>2</sub> Hydrate Formation in the Presence of Acid-Dissolvable Organic Matters. Environmental Science & Technology, 2021, 55, 6206-6213.	4.6	70
23	The Controlling Factors and Ion Exclusion Mechanism of Hydrate-Based Pollutant Removal. ACS Sustainable Chemistry and Engineering, 2019, 7, 7932-7940.	3.2	68
24	Hydrate-bearing sediment of the South China Sea: Microstructure and mechanical characteristics. Engineering Geology, 2022, 307, 106782.	2.9	67
25	Three-body aggregation of guest molecules as a key step in methane hydrate nucleation and growth. Communications Chemistry, 2022, 5, .	2.0	58
26	Organics-Coated Nanoclays Further Promote Hydrate Formation Kinetics. Journal of Physical Chemistry Letters, 2021, 12, 3464-3467.	2.1	57
27	Assessment of gas production from natural gas hydrate using depressurization, thermal stimulation and combined methods. RSC Advances, 2016, 6, 47357-47367.	1.7	56
28	Comparative analysis of the consolidation and shear behaviors of CH4 and CO2 hydrate-bearing silty sediments. Journal of Natural Gas Science and Engineering, 2020, 75, 103157.	2.1	56
29	Effects of Additive Mixture (THF/SDS) on the Thermodynamic and Kinetic Properties of CO <sub>2</sub> /H <sub>2</sub> Hydrate in Porous Media. Industrial & Engineering Chemistry Research, 2013, 52, 4911-4918.	1.8	53
30	The effects of methane hydrate dissociation at different temperatures on the stability of porous sediments. Journal of Petroleum Science and Engineering, 2016, 147, 77-86.	2.1	53
31	Numerical Simulation of the Gas Production Behavior of Hydrate Dissociation by Depressurization in Hydrate-Bearing Porous Medium. Energy & Fuels, 2012, 26, 1681-1694.	2.5	52
32	Experimental Study of Conditions for Methane Hydrate Productivity by the CO <sub>2</sub> Swap Method. Energy & Fuels, 2015, 29, 6887-6895.	2.5	52
33	Numerical Simulation of Methane Production from Hydrates Induced by Different Depressurizing Approaches. Energies, 2012, 5, 438-458.	1.6	49
34	A microfocus x-ray computed tomography based gas hydrate triaxial testing apparatus. Review of Scientific Instruments, 2019, 90, 055106.	0.6	49
35	Hydrate slurry flow characteristics influenced by formation, agglomeration and deposition in a fully visual flow loop. Fuel, 2020, 277, 118066.	3.4	48
36	In-situ visual observation for the formation and dissociation of methane hydrates in porous media by magnetic resonance imaging. Magnetic Resonance Imaging, 2015, 33, 485-490.	1.0	45

#	Article	IF	CITATIONS
37	Experimental measurements of mechanical properties of carbon dioxide hydrate-bearing sediments. Marine and Petroleum Geology, 2013, 46, 201-209.	1.5	44
38	Poreâ€5cale 3D Morphological Modeling and Physical Characterization of Hydrateâ€Bearing Sediment Based on Computed Tomography. Journal of Geophysical Research: Solid Earth, 2020, 125, e2020JB020570.	1.4	44
39	Characteristics of CO2 Hydrate Formation and Dissociation in Glass Beads and Silica Gel. Energies, 2012, 5, 925-937.	1.6	43
40	Visualization of CO2 and oil immiscible and miscible flow processes in porous media using NMR micro-imaging. Petroleum Science, 2011, 8, 183-193.	2.4	42
41	Hydrate-based heavy metal separation from aqueous solution. Scientific Reports, 2016, 6, 21389.	1.6	42
42	Strength behaviors of CH4 hydrate-bearing silty sediments during thermal decomposition. Journal of Natural Gas Science and Engineering, 2019, 72, 103031.	2.1	41
43	Deformation behaviors of hydrate-bearing silty sediment induced by depressurization and thermal recovery. Applied Energy, 2020, 276, 115468.	5.1	40
44	Pressure and Temperature Dependence of Contact Angles for CO <sub>2</sub> /Water/Silica Systems Predicted by Molecular Dynamics Simulations. Energy & Fuels, 2016, 30, 5027-5034.	2.5	39
45	Combined replacement and depressurization methane hydrate recovery method. Energy Exploration and Exploitation, 2016, 34, 129-139.	1.1	38
46	In Situ Local Contact Angle Measurement in a CO <sub>2</sub> –Brine–Sand System Using Microfocused X-ray CT. Langmuir, 2017, 33, 3358-3366.	1.6	38
47	Analysis of the Physical Properties of Hydrate Sediments Recovered from the Pearl River Mouth Basin in the South China Sea: Preliminary Investigation for Gas Hydrate Exploitation. Energies, 2017, 10, 531.	1.6	37
48	Pure methane, carbon dioxide, and nitrogen adsorption on anthracite from China over a wide range of pressures and temperatures: experiments and modeling. RSC Advances, 2015, 5, 52612-52623.	1.7	35
49	Interfacial tension and contact angle measurements for the evaluation of <scp>CO</scp> <sub>2</sub> â€prine twoâ€phase flow characteristics in porous media. Environmental Progress and Sustainable Energy, 2015, 34, 1756-1762.	1.3	35
50	Experimental study on the mechanical properties of sediments containing CH4 and CO2 hydrate mixtures. Journal of Natural Gas Science and Engineering, 2016, 32, 20-27.	2.1	35
51	Lattice Boltzmann Simulation of Growth and Deformation for a Rising Vapor Bubble Through Superheated Liquid. Numerical Heat Transfer; Part A: Applications, 2009, 55, 381-400.	1.2	34
52	Direct Observation of THF Hydrate Formation in Porous Microstructure Using Magnetic Resonance Imaging. Energies, 2012, 5, 898-910.	1.6	34
53	Effect of thermal formation/dissociation cycles on the kinetics of formation and pore-scale distribution of methane hydrates in porous media: a magnetic resonance imaging study. Sustainable Energy and Fuels, 2021, 5, 1567-1583.	2.5	34
54	Analyzing the Process of Gas Production from Methane Hydrate via Nitrogen Injection. Industrial & Engineering Chemistry Research, 2017, 56, 7585-7592.	1.8	33

#	Article	IF	CITATIONS
55	Effect of Temperature on the Mechanical Properties of Hydrate-Bearing Sand under Different Confining Pressures. Energy & Fuels, 2021, 35, 4106-4117.	2.5	33
56	Quantifying the Role of Nanotubes in Nano:Nano Composite Supercapacitor Electrodes. Advanced Energy Materials, 2018, 8, 1702364.	10.2	33
57	Evaluation of Gas Production from Methane Hydrate Sediments with Heat Transfer from Over-Underburden Layers. Energy & Fuels, 2015, 29, 1028-1039.	2.5	32
58	Triaxial tests on the overconsolidated methane hydrate-bearing clayey-silty sediments. Journal of Petroleum Science and Engineering, 2021, 206, 109035.	2.1	32
59	CO <sub>2</sub> Hydrate Formation Characteristics in a Water/Brine-Saturated Silica Gel. Industrial & Engineering Chemistry Research, 2014, 53, 10753-10761.	1.8	31
60	Triboelectric Nanogenerator Powered Electrowetting-on-Dielectric Actuator for Concealed Aquatic Microbots. ACS Nano, 2020, 14, 15394-15402.	7.3	31
61	Quantitative determination of poreâ€structure change and permeability estimation under hydrate phase transition by NMR. AICHE Journal, 2020, 66, e16859.	1.8	30
62	Gas Production Enhancement from a Multilayered Hydrate Reservoir in the South China Sea by Hydraulic Fracturing. Energy & Fuels, 2021, 35, 12104-12118.	2.5	30
63	Estimation of minimum miscibility pressure (MMP) of CO2 and liquid n-alkane systems using an improved MRI technique. Magnetic Resonance Imaging, 2016, 34, 97-104.	1.0	29
64	Permeability estimation of porous media by using an improved capillary bundle model based on micro-CT derived pore geometries. Heat and Mass Transfer, 2017, 53, 49-58.	1.2	29
65	Effects of water-gas two-phase flow on methane hydrate dissociation in porous media. Fuel, 2019, 255, 115637.	3.4	29
66	Magnetic resonance imaging study on near miscible supercritical CO2 flooding in porous media. Physics of Fluids, 2013, 25, .	1.6	28
67	Unstable Densityâ€Driven Convection of CO <sub>2</sub> in Homogeneous and Heterogeneous Porous Media With Implications for Deep Saline Aquifers. Water Resources Research, 2021, 57, e2020WR028132.	1.7	28
68	Formation of Methane Hydrate in Oil–Water Emulsion Governed by the Hydrophilic and Hydrophobic Properties of Non-Ionic Surfactants. Energy & Fuels, 2019, 33, 5777-5784.	2.5	27
69	Wettability of Supercritical CO <sub>2</sub> –Brine–Mineral: The Effects of Ion Type and Salinity. Energy & Fuels, 2017, 31, 7317-7324.	2.5	26
70	In-situ observation for formation and dissociation of carbon dioxide hydrate in porous media by magnetic resonance imaging. Science China Earth Sciences, 2013, 56, 611-617.	2.3	25
71	Measurement of Interfacial Tension of CO <sub>2</sub> and NaCl Aqueous Solution over Wide Temperature, Pressure, and Salinity Ranges. Journal of Chemical & Engineering Data, 2017, 62, 1036-1046.	1.0	25
72	Review: Approaches to research on CO2/brine two-phase migration in saline aquifers. Hydrogeology Journal, 2015, 23, 1-18.	0.9	24

#	Article	IF	CITATIONS
73	Adsorption isotherms and kinetics of carbon dioxide on Chinese dry coal over a wide pressure range. Adsorption, 2015, 21, 53-65.	1.4	24
74	Analyzing spatially and temporally visualized formation behavior of methane hydrate in unconsolidated porous media. Magnetic Resonance Imaging, 2019, 61, 224-230.	1.0	23
75	In-situ observation for natural gas hydrate in porous medium: Water performance and formation characteristic. Magnetic Resonance Imaging, 2020, 65, 166-174.	1.0	23
76	Growth Kinetics and Gas Diffusion in Formation of Gas Hydrates from Ice. Journal of Physical Chemistry C, 2020, 124, 12999-13007.	1.5	23
77	Mechanical behaviors of hydrate-bearing sediment with different cementation spatial distributions at microscales. IScience, 2021, 24, 102448.	1.9	23
78	Quantifying the dynamic density driven convection in high permeability packed beds. Magnetic Resonance Imaging, 2017, 39, 168-174.	1.0	22
79	CO <sub>2</sub> sequestration in depleted methane hydrate deposits with excess water. International Journal of Energy Research, 2018, 42, 2536-2547.	2.2	21
80	Model Comparison of the CH <sub>4</sub> /CO <sub>2</sub> /Water System in Predicting Dynamic and Interfacial Properties. Journal of Chemical & Engineering Data, 2019, 64, 2464-2474.	1.0	21
81	A hydrate blockage detection apparatus for gas pipeline using ultrasonic focused transducer and its application on a flow loop. Energy Science and Engineering, 2020, 8, 1770-1780.	1.9	21
82	Minimum miscibility pressure estimation for a CO2/n-decane system in porous media by X-ray CT. Experiments in Fluids, 2015, 56, 1.	1.1	20
83	Creep Behaviors of Methane Hydrate-Bearing Frozen Sediments. Energies, 2019, 12, 251.	1.6	20
84	Adsorption isotherms and kinetic characteristics of methane on block anthracite over a wide pressure range. Journal of Energy Chemistry, 2015, 24, 245-256.	7.1	19
85	Pore‣cale Imaging and Analysis of Phase Topologies and Displacement Mechanisms for CO <sub>2</sub> â€Brine Twoâ€Phase Flow in Unconsolidated Sand Packs. Water Resources Research, 2017, 53, 9127-9144.	1.7	19
86	Mechanical properties of methane hydrate-bearing sandy sediments under various temperatures and pore pressures. Journal of Petroleum Science and Engineering, 2022, 208, 109474.	2.1	19
87	CO <sub>2</sub> /water two-phase flow in a two-dimensional micromodel of heterogeneous pores and throats. RSC Advances, 2016, 6, 73897-73905.	1.7	18
88	Displacement front behavior of near miscible CO 2 flooding in decane saturated synthetic sandstone cores revealed by magnetic resonance imaging. Magnetic Resonance Imaging, 2017, 37, 171-178.	1.0	18
89	Forced Convection Heat Transfer in Porous Structure: Effect of Morphology on Pressure Drop and Heat Transfer Coefficient. Journal of Thermal Science, 2021, 30, 363-393.	0.9	18
90	Viscosity investigation on metastable hydrate suspension in oil-dominated systems. Chemical Engineering Science, 2021, 238, 116608.	1.9	18

#	Article	IF	CITATIONS
91	Molecular simulations on the stability and dynamics of bulk nanobubbles in aqueous environments. Physical Chemistry Chemical Physics, 2021, 23, 27533-27542.	1.3	18
92	Poreâ€scale contact angle measurements of CO <sub>2</sub> –brine–glass beads system using microâ€focused Xâ€ray computed tomography. Micro and Nano Letters, 2016, 11, 524-527.	0.6	17
93	Strength behaviours of methane hydrate-bearing marine sediments in the South China Sea. Journal of Natural Gas Science and Engineering, 2022, 100, 104476.	2.1	17
94	A novel apparatus for <i>in situ</i> measurement of thermal conductivity of hydrate-bearing sediments. Review of Scientific Instruments, 2015, 86, 085110.	0.6	16
95	Investigation of the Stress–Strain and Strength Behaviors of Ice Containing Methane Hydrate. Journal of Cold Regions Engineering - ASCE, 2012, 26, 149-159.	0.5	15
96	Hydrate phase equilibrium for CH <sub>4</sub> O <sub>2</sub> â€H <sub>2</sub> O system in porous media. Canadian Journal of Chemical Engineering, 2016, 94, 1592-1598.	0.9	15
97	Morphology-Based Kinetic Study of the Formation of Carbon Dioxide Hydrates with Promoters. Energy & Fuels, 2020, 34, 7307-7315.	2.5	15
98	Poreâ€scale investigation of effects of heterogeneity on CO <sub>2</sub> geological storage using stratified sand packs. , 2017, 7, 972-987.		14
99	Creep behaviours of methane hydrate-bearing sediments. Environmental Geotechnics, 2022, 9, 199-209.	1.3	14
100	Strength Behaviors of Remolded Hydrate-Bearing Marine Sediments in Different Drilling Depths of the South China Sea. Energies, 2019, 12, 253.	1.6	14
101	Mechanical Characteristics of the Hydrate-Bearing Sediments in the South China Sea Using a Multistage Triaxial Loading Test. Energy & Fuels, 2021, 35, 4127-4137.	2.5	14
102	MXene (Ti <sub>3</sub> C <sub>2</sub> T <sub><i>x</i></sub> ) as a Promising Substrate for Methane Storage via Enhanced Gas Hydrate Formation. Journal of Physical Chemistry Letters, 2021, 12, 6622-6627.	2.1	14
103	A numerical investigation on the mechanical properties of hydrate-bearing sand using Distinct Element Method. Journal of Natural Gas Science and Engineering, 2021, 96, 104328.	2.1	14
104	Density Measurement and PC-SAFT/tPC-PSAFT Modeling of the CO <sub>2</sub> + H <sub>2</sub> O System over a Wide Temperature Range. Journal of Chemical & Engineering Data, 2014, 59, 1400-1410.	1.0	13
105	Review of Density Measurements and Predictions of CO <sub>2</sub> –Alkane Solutions for Enhancing Oil Recovery. Energy & Fuels, 2021, 35, 2914-2935.	2.5	13
106	Effects of Halogen Ions on Phase Equilibrium of Methane Hydrate in Porous Media. International Journal of Thermophysics, 2012, 33, 821-830.	1.0	12
107	In situ measurement of the dispersion coefficient of liquid/supercritical CO <sub>2</sub> –CH <sub>4</sub> in a sandpack using CT. RSC Advances, 2016, 6, 42367-42376.	1.7	12
108	Strength and Deformation Behaviors of Methane Hydrate-Bearing Marine Sediments in the South China Sea during Depressurization. Energy & Fuels, 2021, 35, 14569-14579.	2.5	12

#	Article	IF	CITATIONS
109	Consolidation deformation of hydrate-bearing sediments: A pore-scale computed tomography investigation. Journal of Natural Gas Science and Engineering, 2021, 95, 104184.	2.1	12
110	Permeability Analysis of Hydrate-Bearing Sediments during the Hydrate Formation Process. Energy & Fuels, 2021, 35, 19606-19613.	2.5	12
111	Analysis of the 3D zone of flow establishment from a ship's propeller. KSCE Journal of Civil Engineering, 2012, 16, 465-477.	0.9	11
112	Behavior of CO 2 /water flow in porous media for CO 2 geological storage. Magnetic Resonance Imaging, 2017, 37, 100-106.	1.0	11
113	Pressure pulse wave attenuation model coupling waveform distortion and viscous dissipation for blockage detection in pipeline. Energy Science and Engineering, 2020, 8, 260-265.	1.9	11
114	Behaviors of NaCl Ions Intruding into Methane Hydrate under a Static Electric Field. Journal of Physical Chemistry C, 2021, 125, 18483-18493.	1.5	11
115	Stress behavior of hydrate-bearing sands with changing temperature and hydrate saturation. Journal of Natural Gas Science and Engineering, 2022, 98, 104389.	2.1	11
116	Molecular dynamics simulation studies of cryoprotective agent solutions: the relation between melting temperature and the ratio of hydrogen bonding acceptor to donor number. Molecular Physics, 2009, 107, 673-684.	0.8	10
117	Measurements of CO <sub>2</sub> –H <sub>2</sub> O–NaCl Solution Densities over a Wide Range of Temperatures, Pressures, and NaCl Concentrations. Journal of Chemical & Engineering Data, 2013, 58, 3342-3350.	1.0	10
118	Dynamic stability characteristics of fluid flow in CO <sub>2</sub> miscible displacements in porous media. RSC Advances, 2015, 5, 34839-34853.	1.7	10
119	Characterization of dissolution process during brine injection in Berea sandstones: an experiment study. RSC Advances, 2016, 6, 114320-114328.	1.7	10
120	A rapid method for the measurement and estimation of CO2 diffusivity in liquid hydrocarbon-saturated porous media using MRI. Magnetic Resonance Imaging, 2016, 34, 437-441.	1.0	10
121	CO <sub>2</sub> diffusion in n-hexadecane investigated using magnetic resonance imaging and pressure decay measurements. RSC Advances, 2014, 4, 50180-50187.	1.7	9
122	Application of X-ray CT investigation of CO2–brine flow in porous media. Experiments in Fluids, 2015, 56, 1.	1.1	9
123	Competitive adsorption/desorption of CO2/CH4 mixtures on anthracite from China over a wide range of pressures and temperatures. RSC Advances, 2016, 6, 98588-98597.	1.7	9
124	New model for particle removal from surface in presence of deformed liquid bridge. Journal of Colloid and Interface Science, 2020, 562, 268-272.	5.0	9
125	Enhanced Mass Transfer by Density-Driven Convection during CO <sub>2</sub> Geological Storage. Industrial & Engineering Chemistry Research, 2020, 59, 9300-9309.	1.8	9
126	A visualization study on two-phase gravity drainage in porous media by using magnetic resonance imaging. Magnetic Resonance Imaging, 2016, 34, 855-863.	1.0	8

#	Article	IF	CITATIONS
127	Effects of Multiple Factors on Methane Hydrate Reformation in a Porous Medium. ChemistrySelect, 2017, 2, 6030-6035.	0.7	8
128	Diffusion Properties for CO <sub>2</sub> –Brine System under Sequestration-Related Pressures with Consideration of the Swelling Effect and Interfacial Area. Industrial & Engineering Chemistry Research, 0, , .	1.8	7
129	Equivalency and Replaceability between Different Permeability Models of Hydrate-Bearing Porous Media When Applied to Numerical Modeling of Hydrate Dissociation: Implications for Model Selection and Parameter Assignment. Energy & Fuels, 2021, 35, 6090-6100.	2.5	7
130	Molecular Insight into the Extraction Behaviors of Confined Heavy Oil in the Nanopore by CO <sub>2</sub> /C <sub>3</sub> H <sub>8</sub> in Huff-n-Puff Process. Energy & Fuels, 2022, 36, 3062-3075.	2.5	7
131	Magnetically Recyclable â^'SO <sub>3</sub> <sup>–</sup> -Coated Nanoparticles Promote Gas Storage via Forming Hydrates. ACS Applied Materials & Interfaces, 2022, 14, 33141-33150.	4.0	7
132	Hydrogen bonds at silica–CO <sub>2</sub> saturated water interface under geologic sequestration conditions. Molecular Physics, 2016, 114, 2924-2935.	0.8	6
133	Solar radiation transfer and performance analysis for a low concentrating photovoltaic/thermal system. Environmental Progress and Sustainable Energy, 2016, 35, 263-270.	1.3	6
134	Experimental study of two-phase flow properties of CO <sub>2</sub> containing N <sub>2</sub> in porous media. RSC Advances, 2016, 6, 59360-59369.	1.7	6
135	Density Measurement and Modeling of CO <sub>2</sub> â^Brine System at Temperature and Pressure Corresponding to Storage Conditions. Journal of Chemical & Engineering Data, 2016, 61, 873-880.	1.0	6
136	Dynamic Adsorption of CO <sub>2</sub> in Different Sized Shale Organic Pores Using Molecular Dynamic Simulations under Various Pressures. Energy & Fuels, 2021, 35, 15950-15961.	2.5	6
137	Experimental Study on the Density-Driven Convective Mixing of CO <sub>2</sub> and Brine at Reservoir Temperature and Pressure Conditions. Energy & Fuels, 2022, 36, 10261-10268.	2.5	6
138	Study of the fluid flow characteristics in a porous medium for CO2 geological storage using MRI. Magnetic Resonance Imaging, 2014, 32, 574-584.	1.0	5
139	MRI investigation of water–oil two phase flow in straight capillary, bifurcate channel and monolayered glass bead pack. Magnetic Resonance Imaging, 2015, 33, 918-926.	1.0	5
140	Visualization of asphaltene deposition effects on porosity and permeability during CO2 flooding in porous media. Journal of Visualization, 2016, 19, 603-614.	1.1	5
141	Magnetic-resonance imaging and simplified Kozeny-Carman-model analysis of glass-bead packs as a frame of reference to study permeability of reservoir rocks. Hydrogeology Journal, 2017, 25, 1465-1476.	0.9	5
142	Visualization study on the promotion of depressurization and water flow erosion for gas hydrate production. Energy Procedia, 2019, 158, 5563-5568.	1.8	5
143	Effects of Pore Structures on Seepage and Dispersion Characteristics during CO2 Miscible Displacements in Unconsolidated Cores. Energy & Fuels, 0, , .	2.5	5
144	Evidence of Guest–Guest Interaction in Clathrates Based on <i>In Situ</i> Raman Spectroscopy and Density Functional Theory. Journal of Physical Chemistry Letters, 2022, 13, 400-405.	2.1	5

#	Article	IF	CITATIONS
145	Molecular behavior of hybrid gas hydrate nucleation: separation of soluble H <sub>2</sub> S from mixed gas. Physical Chemistry Chemical Physics, 2022, 24, 9509-9520.	1.3	5
146	Fractal dimension analysis on pore structure of artificial cores using magnetic resonance imaging. , 2012, , .		4
147	Experimental investigation on spontaneous counterâ€current imbibition in waterâ€wet natural reservoir sandstone core using MRI. Magnetic Resonance in Chemistry, 2017, 55, 546-552.	1.1	4
148	Non-Embedded Ultrasonic Detection for Pressure Cores of Natural Methane Hydrate-Bearing Sediments. Energies, 2019, 12, 1997.	1.6	4
149	The Study of Flow Characteristics During the Decomposition Process in Hydrate-Bearing Porous Media Using Magnetic Resonance Imaging. Energies, 2019, 12, 1736.	1.6	4
150	Molecular simulation of equal density temperature in CCS under geological sequestration conditions. , 2020, 10, 90-102.		4
151	Ultralow thermal conductivity in tetrahydrofuran clathrate hydrate. Applied Physics Letters, 2021, 119, .	1.5	4
152	Three-Dimensional Thermal Simulations of 18650 Lithium-Ion Batteries Cooled by Different Schemes under High Rate Discharging and External Shorting Conditions. Energies, 2021, 14, 6986.	1.6	4
153	Heat value identification of coal in utility boilers with neural network. , 2010, , .		3
154	Measurement of gas diffusion coefficient in liquid-saturated porous media using magnetic resonance imaging. Russian Journal of Physical Chemistry A, 2014, 88, 2265-2270.	0.1	3
155	Tetrahydrofuran hydrate decomposition characteristics in porous media. Russian Journal of Physical Chemistry A, 2016, 90, 2377-2382.	0.1	3
156	Interrelationship between water film thicknesses and contact angles and a model for CO2 adhesion. Molecular Simulation, 2019, 45, 868-875.	0.9	3
157	Fast Peelâ€Off Ultrathin, Transparent, and Freeâ€Standing Films Assembled from Lowâ€Dimensional Materials Using MXene Sacrificial Layers and Produced Bubbles. Small Methods, 2021, , 2101388.	4.6	3
158	An experiment study on fluid heat and mass transfer properties in porous media using MRI. Russian Journal of Physical Chemistry A, 2014, 88, 2214-2219.	0.1	2
159	Density measurement and equal density temperature of CO2+brine from Dagang — formation from 313 to 363 K. Korean Journal of Chemical Engineering, 2015, 32, 141-148.	1.2	2
160	CO <sub>2</sub> capillary trapping behaviour in glass sand packed heterogeneous porous media during drainage and imbibition revealed by magnetic resonance imaging. RSC Advances, 2016, 6, 101452-101461.	1.7	2
161	Displacement and Dissolution Characteristics of CO \$\$_{2}\$\$ 2 /Brine System in Unconsolidated Porous Media. Transport in Porous Media, 2018, 122, 595-609.	1.2	2
162	Progress on Laboratory-Scale Reactors for Simulating Gas Production from Hydrate Reservoir. Energy & Fuels, 2021, 35, 16416-16431.	2.5	1

#	Article	IF	CITATIONS
163	Synchronous observation of rising soluble bubble through quiescent solution. Frontiers of Energy and Power Engineering in China, 2009, 3, 307-312.	0.4	0
164	Indoor Analogue Tests for High Temperature Heat Pump and Its Industrial Application. , 2010, , .		0
165	Numerical simulation of heat transfer effects on methane hydrate dissociation by depressurization. , 2012, , .		0
166	Experiment Study on Temperature Distribution in Water-Saturated Porous Media. Applied Magnetic Resonance, 2015, 46, 793-808.	0.6	0
167	Noninvasive temperature and velocity mapping using magnetic resonance imaging. Journal of Visualization, 2016, 19, 403-415.	1.1	0